iScience

CellPress
OPEN ACCESS

Article

Preclinical efficacy of TZG in myofascial pain syndrome by impairing PI3K-RAC2 signaling-mediated neutrophil extracellular traps

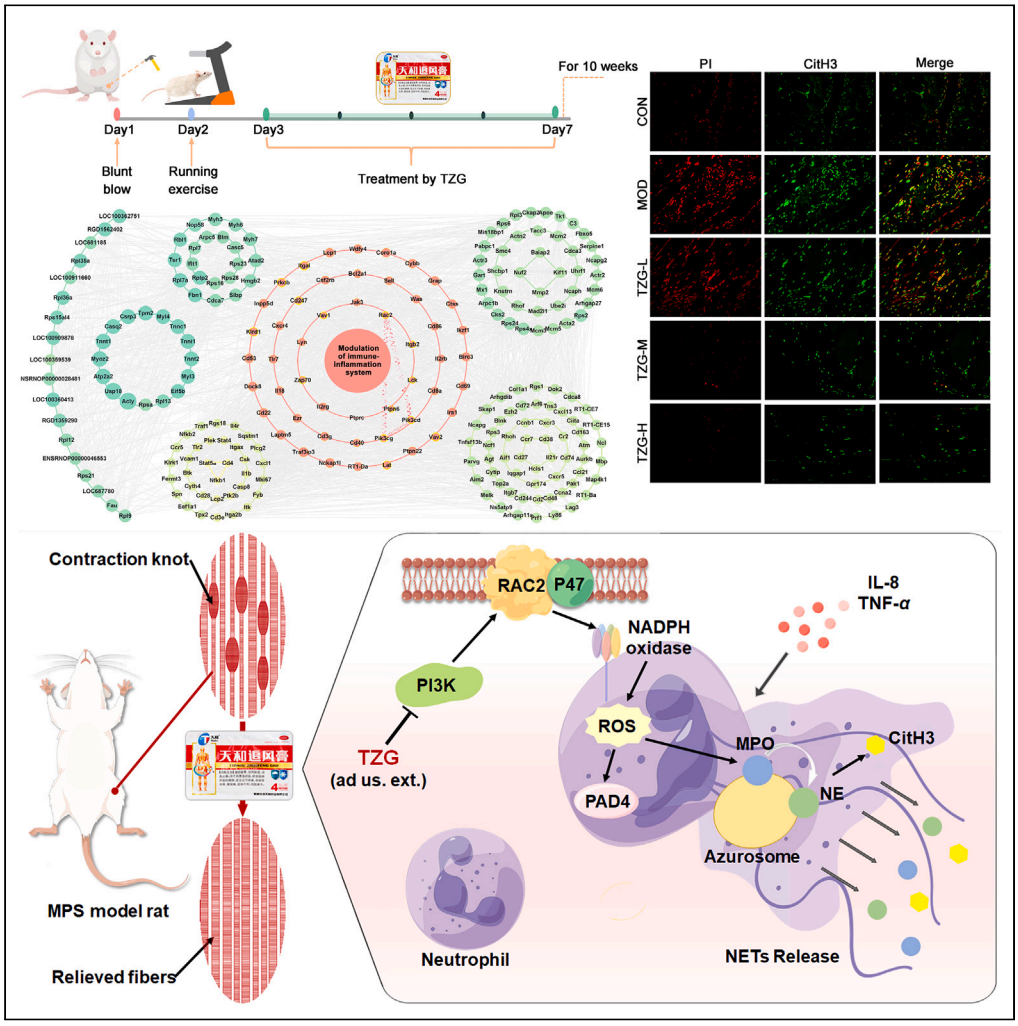

Xueting Liu, Xia Mao, Yudong Liu, Wenjia Chen, Weijie Li, Na Lin, Yanqiong Zhang

yqzhang@icmm.ac.cn (Y.Z.)
nlin@icmm.ac.cn (N.L.)

Highlights

TZG treatment obviously alleviated disease severity of MPS rats

TZG may impair PI3K-RAC2 axis-mediated NETs formed in MPS rats

This study shed light into broadening the clinical indications of TZG

Liu et al., iScience *26*, 108074
October 20, 2023
https://doi.org/10.1016/j.isci.2023.108074

iScience

CellPress
OPEN ACCESS

Article

Preclinical efficacy of TZG in myofascial pain syndrome by impairing PI3K-RAC2 signaling-mediated neutrophil extracellular traps

Xueting Liu,[1,2] Xia Mao,[1,2] Yudong Liu,[1,2] Wenjia Chen,[1] Weijie Li,[1] Na Lin,[1,*] and Yanqiong Zhang[1,3,*]

SUMMARY

Tianhe Zhuifeng Gao (TZG) shows a satisfying therapeutic efficacy in treating arthromyodynia, which shares similar etiology to myofascial pain syndrome (MPS). We herein aim to explore whether TZG could be a potential prescription for MPS therapy. An MPS rat model was successfully established presenting with reduced pain thresholds, abnormal local switch responses, *etc.*, which was effectively reversed by TZG treatment externally. A transcriptome sequencing based on the active MTrPs samples of rats, combined with network analysis revealed that TZG might ameliorate the progression of MPS by impairing neutrophil extracellular traps (NETs) release through inhibiting PI3K-RAC2 signaling to reduce NADPH oxidase-originated ROS. Experimentally, the expression levels of inducers, biomarkers of NETs formation and vessel injury, and p-PI3K, p-P47, and RAC2 proteins were all significantly up-regulated in affected tissues, which were markedly reversed by TZG. Our results not only shed light into broadening the clinical indications of TZG, but benefit MPS therapy.

INTRODUCTION

Myofascial pain syndrome (MPS) presents as a common disorder with the prevalence varying between 21% and 30% in internal medicine and orthopedics clinics, and even affects as many as 85% of individuals during the lifetime, with variable rates between males and females.[1,2] It is a musculoskeletal condition that stemmed from myofascial trigger points (MTrPs) within localized, taut regions comprised skeletal muscle and fascia.[3] MTrPs are hypersensitive to palpation, leading to the production of a distinct local and referred pain, in consistent with patients' presenting chronic and persistent regional pain involved in shoulder, back, head, and face.[4,5] The pathophysiological characteristics of MTrPs initiation and symptomatology is still under vigorous investigations but is likely multifactorial, arising as a result of trauma or overuse induced muscular injury, aging musculoskeletal degeneration, radiculopathy, spinal sensitization, and at the neuromuscular junction resulting in higher than normal concentrations of acetylcholine and corresponding receptors at the motor endplate.[6] Dysfunctional motor endplates caused sustained muscle fiber contractions, which in turn bring about decreased perfusion of muscle, local muscle ischemia, toxic metabolites accumulation, and pain that were associated with taut bands in muscle.[7] Clinically, the treatment of MPS targets MTrPs for intercepting factors that promoted its formation by correcting structural and mechanical imbalance, including pharmacological treatment modalities (nonsteroidal anti-inflammatory drugs, tri-cyclic antidepressants, muscle relaxants, and *etc.*) and minimally invasive non-pharmacologic treatment options (myofascial release, dry needling, acupuncture, and *etc.*).[8] Simultaneously, a multidisciplinary approach is often applied for maximizing therapeutic potentials for achieving a positive outcome. However, the current therapeutic strategies are not capable of permanently inhibiting the active MTrPs due to the incomplete elimination of underlying etiologic lesion. More effective and patient-friendly medicines are urgently needed to be developed.

New studies increasingly point to the novel use of available drugs (or medications) that may offer new clinical applications with shorter approval processes and lower costs and risks than new drug development based on the *de novo* experiments. Tianhe Zhuifeng Gao (TZG) is a clinically approved Chinese patent medicine (approval number: Z45021872), and consists of twenty-six medicines (*Ephedra*, *Asarum Sieboldii*, *Cinnamomum Cassia*, *Notopterygium Incisum*, *Radix Aconiti*, *Angelica Sinensis*, *etc.*) and nine chemical compounds (eugenol type basil oil, muscone, menthol, methyl salicylate, *etc.*), exerting satisfying clinical efficacies in treating rheumatoid arthritis (RA) and periarthritis of shoulder without toxicity observed.[9] TZG was originally designed for alleviating arthromyodynia, caused by interaction stimuli of wind, cold and damp pathogenic factors, that manifested with rheumatism arthralgia, lumber and back pain, numbness of limbs, and other extension disorders, which may be interestingly similar to the etiology and characteristics of MPS. In clinics, both MPS and RA are the musculoskeletal disorders, due to the occurrence of patients' complaints of pain and tenderness to palpation, which seriously decreased range of motion of the affected muscle.[10]

[1]Research Center of Traditional Chinese Medicine Theory and Literatures, Institute of Chinese Materia Medica, China Academy of Chinese Medical Sciences, Beijing 100700, China
[2]These authors contributed equally
[3]Lead contact
*Correspondence: yqzhang@icmm.ac.cn (Y.Z.), nlin@icmm.ac.cn (N.L.)
https://doi.org/10.1016/j.isci.2023.108074

Depolarization thresholds, neurogenic inflammation, and receptor expression all contribute to the initiation and perpetuation of MPS and RA.[11] The ultimate goal of the current therapeutics, such as nonsteroidal anti-inflammatory drugs and muscle relaxants, is to alleviate the pain and eliminate inflammation.[12,13] Therefore, we hypothesized that TZG might be a potential prescription for MPS therapy.

To verify this hypothesis, we herein established a persistent muscle pain model with MTrPs, which mimics environmental pathogenic factors of MPS through long-term hammering together with continuous running exercise. Then, the electromyogram of MTrPs, the histological changes of muscle, glycosaminoglycans accumulation, and the involved hyperalgesia-related indicators were examined before and after TZG treatment. On the basis of the confirmed therapeutic efficacy, we carried out a transcriptome sequencing using active MTrPs samples of rats, combined with a network analysis and *in vivo* experimental validations, the results of which may offer an evidence to expand the clinical indications of TZG and to benefit MPS therapy.

RESULTS

Pain threshold changes, the number of MTrPs, histomorphological changes, and glycosaminoglycans accumulation in an MPS animal model

An MPS animal model in Sprague-Dawley (SD) rats was established to stimulate the development and progression of this disease in clinics (Figure 1A). The changes in mechanical hyperalgesia and acetone-induced cold allodynia of left vastus medialis with blunt trauma were measured throughout the modeling cycle. Two kinds of pain thresholds of rats in the MPS model group were obviously decreased compared with that in the normal control group, lasting for 10 weeks (all $p < 0.05$, Figures 1B and 1C). Abnormal limb lifting, shaking, gait instability or other pain-related behaviors were not observed in the normal control group (Figures 1B and 1C). Taut band of rats appeared, and MTrPs were identified by applying electromyography (EMG) analysis. In the MPS model group, local switch responses (LTRs) were observed, and spontaneous electrical activity (SEA), presenting by positive sharp waves and fibrillation potentials, appeared continuously for more than 30 s while less than 10 min in taut bands of rats when electrodes were inserted into tant bands on the 8th week, which implied the presence of a MTrP at injured left vastus medialis. However, no positive sharp waves were found in rats of normal control group (Figure 1D). Microscopic analysis of hematoxylin and eosin (H&E) staining revealed that the muscle fibers in the normal control group were uniform in size, polygonal, and regular in arrangement in cross-section. In addition, myofibrils in muscle cells were levelly stained. Conversely, contracture knots presenting as large round muscle cells were observed in the cross-sectional space of MTrPs in the MPS model group indicated by yellow arrow in Figure 2A. Muscle-fiber and -bundle space was both abnormally widened with narrower sarcomeres and continuous expansion of pyramidal muscle fibers, accompanied by mononuclear cells infiltration and nuclear in-migration that mostly moved to the interior or the center of the cells in the longitudinal section (Figure 2A). These alterations in MPS model group were closely associated with structural changes, characterized by the presence of extracellular glycosaminoglycan's around the contraction knots, with some fuchsia coloration indicating the presence of neutral glycosaminoglycan and blue color indicating the presence of acid glycosaminoglycan using Alcian periodic acid Schiff (PAS) staining (Figure 2B). Since neurotrophins have been recognized to be closely associated with the pathogenesis of MPS related pain,[14] nerve growth factor (NGF), and brain-derived neurotrophic factor (BDNF) expression levels in spinal dorsal horn of rats were detected and were found to be significantly enhanced in the MPS model group compared with normal control group (both $p < 0.001$, Figures 1E and 1F). These data suggest that the MPS animal model was successfully established.

TZG effectively alleviated disease severity in MPS animal models

During the experimental procedures, therapeutic interventions with low-, middle-, and high-doses of TZG (TZG-L, TZG-M, TZG-H) significantly increased the mechanical hyperalgesia and acetone-induced cold allodynia of injured left vastus medialis since the 5th week till the 10th week (all $p < 0.05$, Figures 1B and 1C), eliminated LTR and SEA (Figure 1D), recovered atrophy and breakage of muscle cells in MTrP morphology, reduced inflammatory cell infiltration, as well decreased contracture knots in rats of MPS model group (Figure 2). Besides, all three dosages of TZG effectively reduced the expression levels of both NGF and BDNF with statistical significance compared with MPS model group (all $p < 0.05$, Figures 1E and 1F). Notably, the therapeutic effects of TZG were similar to that of positive drug Shexiang Zhuanggu Gao (SXZG), and no obvious differences were observed between normal control groups and all treatment groups in terms of all indicators mentioned earlier (Figures 1 and 2).

PI3K-RAC2 signaling may be one of the pharmacological targets of TZG in alleviating the disease severity of MPS

In view of the confirmed pharmacological effects of TZG on MPS, we would like to investigate the underlying mechanism by integrating transcriptome sequencing and "disease-drug" interaction network analysis. As a result, a total of 931 MPS-related genes (differential expression genes [DEGs] of MPS model group vs. control group, including 762 upregulated and 169 downregulated genes) and 461 TZG effective genes (DEGs of TZG treatment group vs. MPS model group, including 56 upregulated and 405 downregulated genes) were identified. Two volcano plots were created with all the differentially expressed genes (Figure 3A). Then, the "MPS-related genes-TZG effective genes" interaction network was constructed, which consists of 748 gene nodes and 3737 interaction edges. Following evaluating the topological importance of nodes in the network, 239 hub genes, the degree of which were two times higher than the median (the median value is 5) of all genes, were screened, and 2494 pairs of direct interaction among the hub genes were also extracted. According to the shortest path value of each drug hub target-disease hub gene pairs, there were 50 hub genes indicated as the major TZG effective targets against MPS. The detailed information of the shortest path value of each drug hub target-disease hub gene pairs is provided in Table S1.

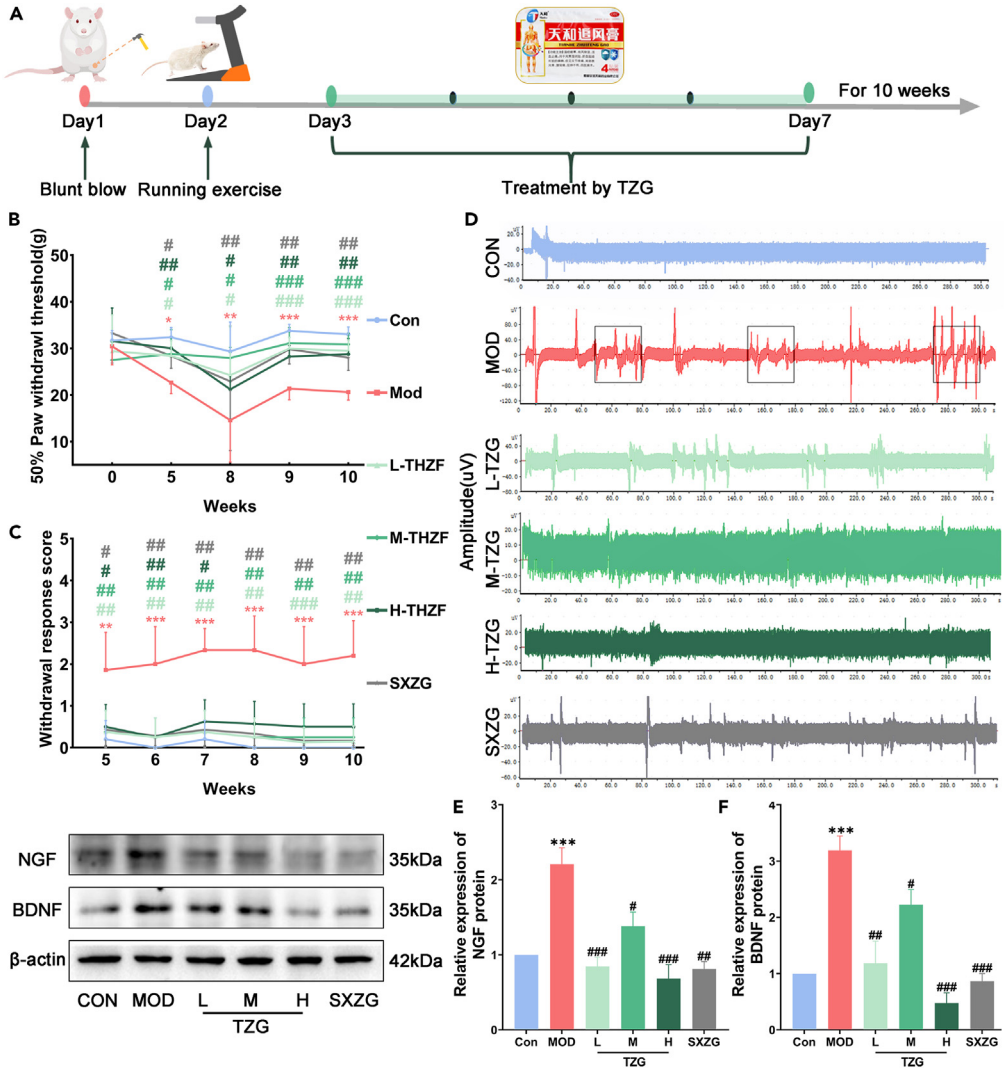

Figure 1. TZG effectively alleviated disease severity in MPS rats by reversing the pain threshold changes, the number of MTrPs and pain-related proteins

(A) Schematic illustration for the experimental design and procedures.

(B) Time course of mechanical hyperalgesia on MTrPs of rats in different groups.

(C) Time course of acetone-induced cold allodynia on MTrPs of rats in different groups.

(D) EMG analysis for detecting SEA on MTrPs of rats in different groups.

(E) Expression levels of NGF protein in vastus medialis muscle around MTrPs of rats in different groups detected by western blot analysis.

(F) Expression levels of BDNF protein in vastus medialis muscle around MTrPs of rats in different groups detected by western blot analysis. The number of rats in each group was 8. Data are expressed as the mean ± S.D. "*," "**," and "***," $p < 0.05$, $p < 0.01$, and $p < 0.001$, respectively, comparison with the normal control group. "#," "##," and "###", $p < 0.05$, $p < 0.01$, and $p < 0.001$, respectively, comparison with the MPS model group.

Functionally, the major TZG effective targets against MPS were significantly involved into the modulation of immune-inflammation system (Figure 3B). Especially, the most enriched 5 pathways were natural killer cell mediated cytotoxicity (hsa04650), T cell receptor signaling pathway (hsa04660), Fc gamma R-mediated phagocytosis (hsa04666), Fc epsilon RI signaling pathway (hsa04664), and B cell receptor signaling pathway (hsa04662) in sequence according to their significance (Figure 3C). Ten genes most frequently enriched in the previous-pathways were provided in Figure 3D. Among them, there were 14 major TZG effective targets against MPS, including PRKCB, ITGB2, PIK3CD, ITGAL, PIK3CG, VAV1, VAV2, ZAP70, LCK, RAC2, KLRD1, PTPN6, CD247, and LAT, involved into the most enriched pathway. Interestingly, PIK3CD [Catalytic subunits of phosphatidylinositol-3-hydroxykinase (PI3K)], PIK3CD/p110δ)/PIK3CG (Catalytic subunits of PI3K, PIK3CD/p110γ) (PI3K)-ras-related C3 botulinum toxin substrate 2 (RAC2) signaling was markedly associated with the formation of neutrophil extracellular traps (NETs) (https://www.kegg.jp/pathway/map04613), which may play a crucial role in various autoimmune and inflammatory diseases.[15–18] NETs mediate tissue damage in various experimental models of autoimmune diseases, leading to the capture and inactivation

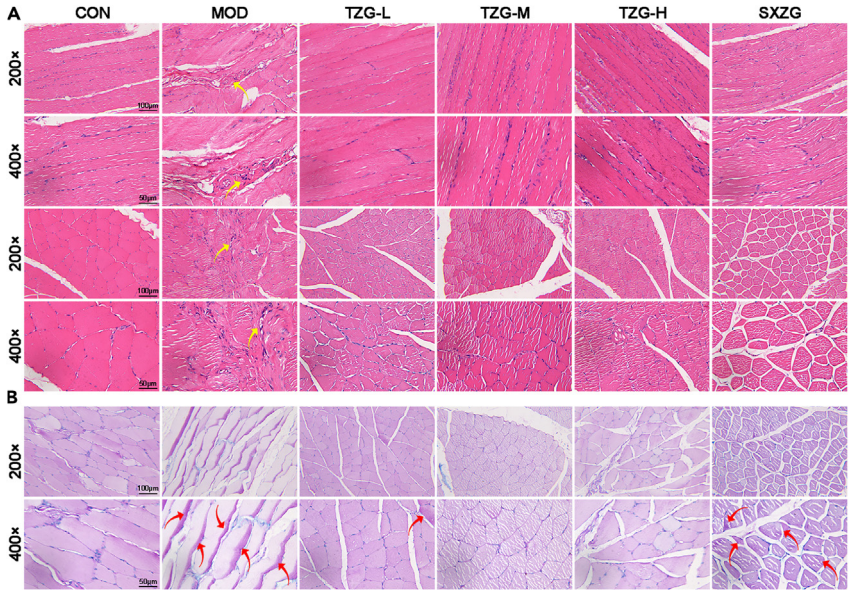

Figure 2. TZG effectively ameliorated the histological changes and glycosaminoglycan accumulation in MPS rats

(A) HE staining of the vastus medialis muscle around marked taut band of rats in different groups showing the histomorphological changes of located tissues at the magnification of 200× and 400× in cross-section (upper), and that in the longitudinal section (down). Yellow arrows indicated pathological sites of MTrPs. (B) Alcian PAS staining of the vastus medialis muscle around marked taut band of rats in different groups showing the histomorphological changes of located tissues at the magnification of 200× (upper) and 400× (down). Fuchsia coloration indicates the presence of neutral glycosaminoglycan and blue color indicates the presence of acid glycosaminoglycan. Red arrows indicated pathological sites of MTrPs. The number of rats in each group was 8.

of pathogens in chronic and debilitating pain.[19] On the basis of the quantitative data obtained from the transcriptome sequencing, the expression levels of PIK3CD, PIK3CG, and RAC2 genes were all up-regulated in MPS rats compared to the normal control group, while were effectively reduced by the treatment of TZG. These data prompt us to hypothesize that PI3K-RAC2 signaling might be one of the pharmacological targets of TZG in alleviating the disease severity of MPS.

TZG impairs NETs release through inhibiting PI3K-RAC2 signaling-mediated nicotinamide adenine dinucleotide phosphate (NADPH) oxidase reactive oxygen species (ROS) production in MPS

To verify the previous hypothesis, we then explore the expression levels of inflammatory inducers [interleukin-8 (IL-8), tumor necrosis factor alpha (TNF-α)], biomarkers of NETs formation [double-stranded deoxyribonucleic acid (dsDNA), myeloperoxidase (MPO), citrullinated histone H3 (CitH3), peptidylarginine deiminase 4 (PAD4)] and vessel injury (CD31), and the corresponding proteins in PI3K-RAC2 signaling (p-PI3K, p-47, RAC2) using the biological samples obtained from rats in different groups. As shown in Figures 4A and 4D, the immunofluorescence of CitH3 in vastus medialis muscle around MTrPs revealed a higher proportion of nuclei positive for CitH3 in the MPS model group comparing with normal control group ($p < 0.001$). Quantification of signal showed a dose-dependent response for propidiumiodide (PI) pixels after TZG treatment (all $p < 0.001$) (Figures 4A and 4D). A stronger CD31 staining in vastus medialis muscle around MTrPs was observed in the MPS model group than that in the normal control group ($p < 0.01$), which was significantly reduced in the TZG treated groups (all $p < 0.01$, Figures 4B and 4G). Additionally, TZG also reversed the abnormal morphology of micro vessel in the MPS model group, suggesting TZG may exert a vascular protective effect (Figures 4B and 4G). Both the expression levels of neutrophil elastase (NE) and PAD4 proteins in the MPS model group were significantly higher than those in the normal control group ($p < 0.05$ and $p < 0.001$, respectively). In contrast, the external administration of TZG to the MTrPs effectively reversed NE and PAD4 protein expression ($p < 0.01$ and $p < 0.001$, respectively, Figures 4C, 4E, and 4F). Quantitative evaluation of Enzyme-linked immunosorbent assay (ELISA) data for dsDNA (Figure 5A), IL-8 (Figure 5B), TNF-α (Figure 5C), and MPO (Figure 5E) indicated the significant increase of these indicators in the MPS model group compared with the normal control group (all $p < 0.001$). Intriguingly, an obvious decrease was observed in the TZG treated groups with a dose-dependent manner (All $p < 0.01$), the trend of which were in accordance with that of CitH3, and similar to its immunofluorescence analysis (Figure 5D). These data demonstrated the successful establishment of MPS animal model and the therapeutic effects of TZG.

Mechanically, the further western blot analysis of the p-PI3K/PI3K and p-P47/P47 ratios, and RAC2 protein expression were performed to validate our hypothesis. As shown in Figures 5F–5I, all the p-PI3K/PI3K and p-P47/P47 ratios, and RAC2 protein expression showed a remarkably increase pattern in the MPS model group comparing with the normal control group (all $p < 0.001$), while significantly reduced after the treatment of TZG (all $p < 0.001$).

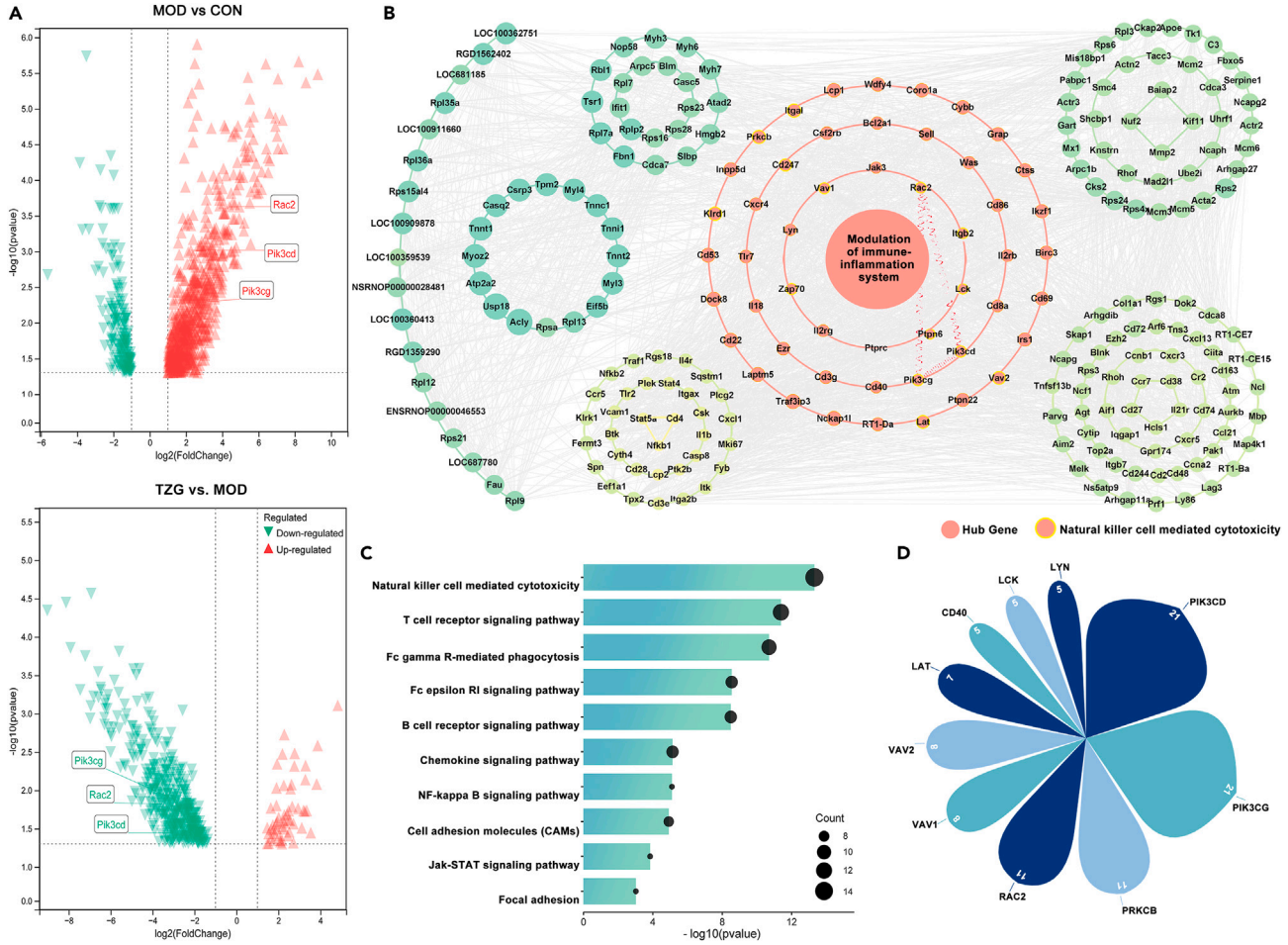

Figure 3. Transcriptome sequencing and network analysis reveals that PI3K-RAC2 signaling may be one of effective targets of TZG in alleviating the disease severity of MPS

(A) Volcano plots show differentially expressed genes (DEGs) between MPS model group vs. normal control group (upper), and between TZG treatment group vs. MPS model group (down). Triangles in red indicate the up-regulated genes, and triangles in green indicate the down-regulated genes.

(B) "MPS-related gene-TZG-effective gene" interaction network was constructed using links between MPS-related genes (DEGs between MPS model group vs. control group) and TZG effective genes (DEGs between TZG treatment group vs. MPS model group). The key hub nodes in the network were significantly enriched in the modulation of immune-inflammation system. Circles in pink indicate hub genes, and those surrounded by yellow indicate genes in natural killer cell mediated cytotoxicity.

(C) Enrichment analysis of top 10 KEGG and Reactome pathways. Size of black dots depicts the count being the strongest evidence of enrichment.

(D) Petals figure of top 10 genes that are most frequently appeared in top 10 enriched pathways.

DISCUSSION

From a musculoskeletal pain perspective, the MPS in initial stages may be triggered by peripheral nociceptor stimuli, which will induce changes in brain networks, and then begin to generate self-inputs to sustain the pain sensation in turn.[20] In other words, it is of central sensitization syndrome, featured with greater disinhibition in the motor cortex and the descending pain inhibitory system than healthy subjects.[14] MTrPs in MPS not only create foci of pain, but presents with a neuropathic component in combination with other neurocutaneous components.[21] Several hypotheses regarding the interaction mechanisms that may underpin the neurogenic origins of MTrPs include peripheral and central sensitization, α-motor neuron discharge and the integrated hypothesis, the latter of which is featured by a feedback loop of abnormal increased acetylcholine release at the motor endplate nerve terminal, sustained muscle fiber contractions, taut band formation, and autonomic modulation.[22] The existing therapeutic strategies for MPS are often conservative and have a problem of poor clinical efficacy.[23] Therefore, the discovery of novel and effective drugs for this disease may be a significant challenge in drug development. Drug repositioning may be an efficient strategy for identifying and developing new usage for existing drugs to reduce the overall cost and shorten the time required to bring new drugs into commerce. In the current study, we focus on the potentials of TZG for treating MPS since it acts as a clinical approved prescription extensively used for the treatment of RA and periarthritis of shoulder with favorable therapeutic effects, and

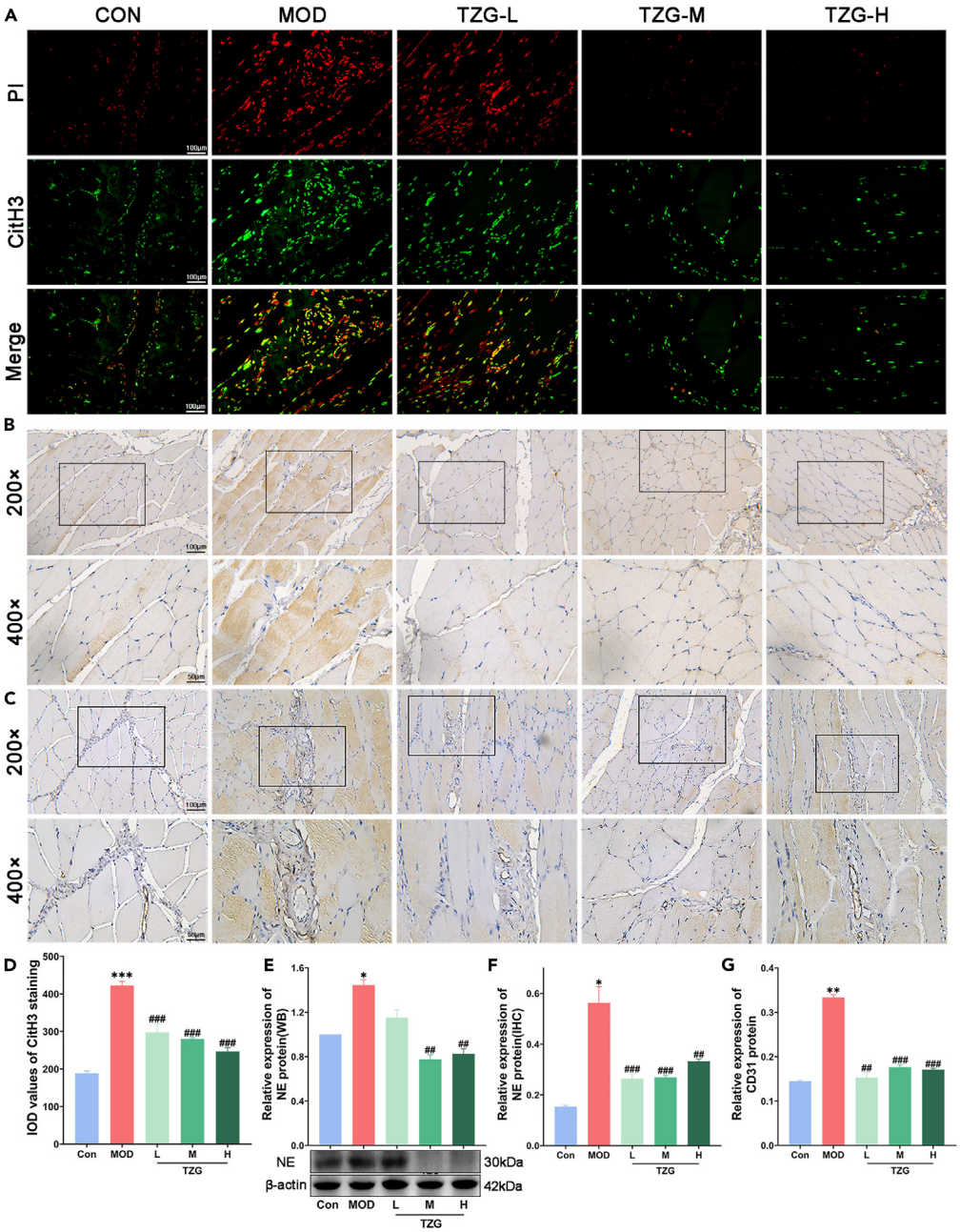

Figure 4. TZG significantly impairs the formation and the release of NETs

(A and D) Immunofluorescence staining of CitH3 protein in vastus medialis muscle around MTrPs of rats in different groups.

(B and G) Immunohistochemistry analysis of CD31 protein in vastus medialis muscle around MTrPs of rats in different groups at the magnification of 200× (upper) and 400× (down).

(C and F) Immunohistochemistry analysis of NE protein in vastus medialis muscle around MTrPs of rats in different groups at the magnification of 200× (upper) and 400× (down).

(E) Expression levels of NE protein in vastus medialis muscle around MTrPs of rats in different groups detected by western blot analysis. The number of rats in each group was 8. Data are expressed as the mean ± S.D. "*," "**," and "***," $p < 0.05$, $p < 0.01$, and $p < 0.001$, respectively, comparison with the normal control group. "#", "##," and "###", $p < 0.05$, $p < 0.01$, and $p < 0.001$, respectively, comparison with the MPS model group.

both RA and MPS are the most common musculoskeletal problems characterized with chronic or acute widespread pain and sharing various invasive or non-invasive treatment modalities.[24] We herein determined whether TZG could exert a therapeutic effect in MPS and also explored the underlying pharmacological mechanisms.

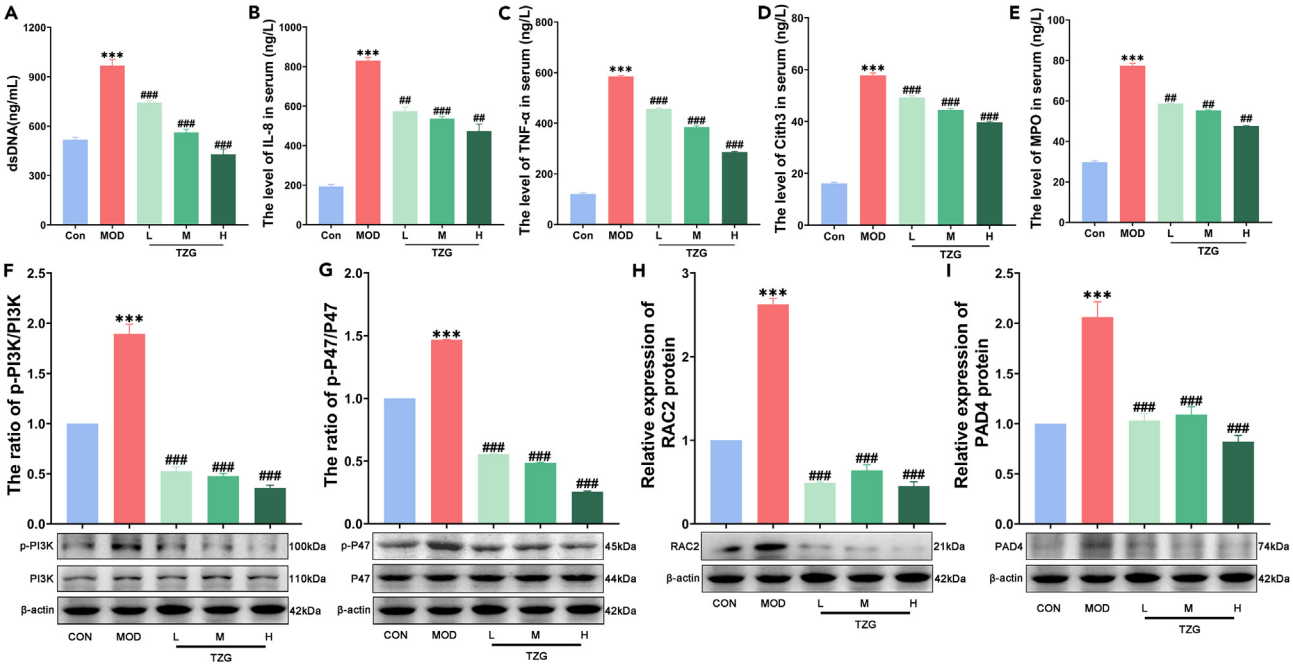

Figure 5. TZG significantly regulated the expression of NETs formation-related indicators, and the corresponding proteins in PI3K-RAC2 signaling

(A–E). Serum levels of dsDNA, IL-8, TNF-α, CitH3, and MPO detected by ELISA analyses, respectively. Samples in (A)∼(E) were obtained from the blood supernatant of rats in different groups.

(F–I) The ratios of p-PI3K/PI3K and p-P47/P47, and the expression levels of RAC2 and PAD4 proteins detected by western blot analyses, respectively. Samples in (F)∼(I) were obtained from MTrPs tissues of rats in different groups. The number of rats in each group was 8. Data are expressed as the mean ± S.D. "*," "**," and "***," $p < 0.05$, $p < 0.01$, and $p < 0.001$, respectively, comparison with the normal control group. "#," "##," and "###," $p < 0.05$, $p < 0.01$, and $p < 0.001$, respectively, comparison with the MPS model group.

We firstly established an MPS animal model, which imitates clinical symptoms and etiology of MPS, for providing a vehicle for evaluating the therapeutic effects of TZG in MPS. Currently, various animal models of muscle pain have been developed, such as inflammatory substances-induced inflammatory muscle pain, eccentric contraction-induced delayed onset muscle soreness, and acidic saline-triggered hyperalgesia model. However, none of which developed a persistent muscle pain that associated with MTrPs.[6] We then adopted an MPS animal model that was previously reported by Huang et al. combining continuous bluntly striking and eccentric-based exercises, which can develop taut band-like muscle hardening, and exhibit referred pain and LTR during needle insertion.[25] Consistently, our MPS rats displayed the lower pain thresholds, abnormal LTR, pathological changes and extracellular glycosaminoglycan in vastus medialis muscle around marked taut band of rats and enhanced expression levels of nociceptive transmission-related proteins NGF and BDNF, which can mediate the disinhibition of motor cortex excitability, as well as the function of descending inhibitory pain modulation system, independently of the physiopathology mechanism involved in these musculoskeletal pain syndromes.[14] These are in accord to the diagnostic criteria of MPS including the regional hypersensitive spot in muscle, the appearance of palpable taut band, the referred pain and current pain complaint evoked by palpation on MTrPs.[26] Our data demonstrated that TZG treatment obviously reversed the abnormal changes of MPS rats to a nearly normal level, similar to that of the positive drug SXZG. Following the transcriptome sequencing, the "disease-related gene-drug effective target" interaction network based on transcriptomic data were constructed and the major TZG effective targets against MPS were screened according to the topological importance. Further functional investigation revealed that the major TZG effective targets were significantly enriched in the modulation of immune-inflammation system, and PI3K-RAC2 signaling-mediated NADPH oxidase reactive oxygen species (ROS) production and impairing NETs release might be one of the therapeutic targets of TZG against MPS.

When stimulated with particular matter and certain chemicals, the inflammatory responses are occurred immediately after tissue damage or a sense of pain, and the immune-inflammation system is subsequently activated to eliminate dead and devitalized tissues, characterized with a sustained influx of neutrophils and persistent NETs release.[27] Especially, NETs are defined as decondensed chromatin web-like structures formed mainly depending on NADPH oxidase-originated oxidative burst of ROS by extrusion of decondensed DNA chromatin into the extracellular space complexed with CitH3, together with various neutrophil-derived proteins such as MPO, PAD4, NE, and dsDNA. The enzymatic activities of MPO and NE have been reported to contribute to antibacterial activity or tissue damage. PAD4 participate in NETs mediated antibacterial innate immunity, and dsDNA that normally contained in nuclei can be recognized as a damage associated molecular patterns during inflammatory responses.[28] NETs expel from neutrophils not only for trapping and degrading microorganism, but playing a pivotal role in the host killing capacity during inflammation. However, the excessive release of NETs may damage healthy tissues.[29] In this

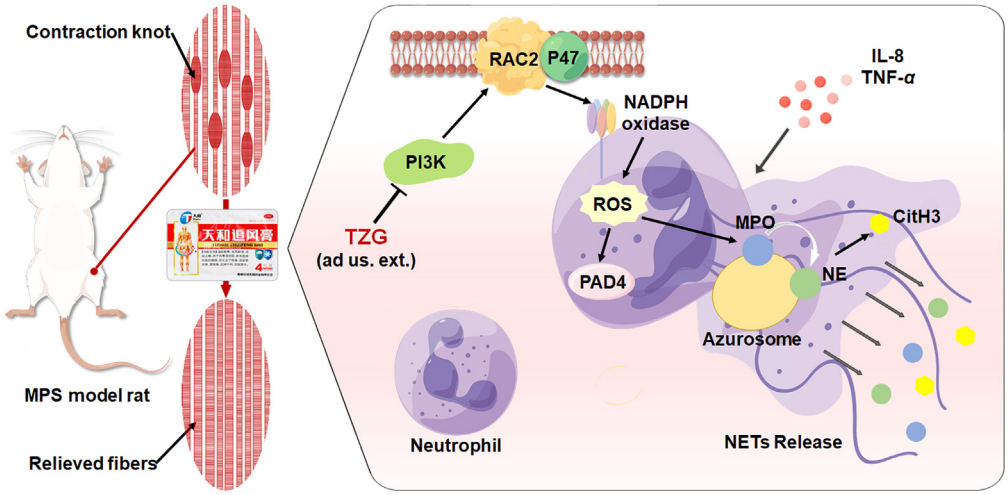

Figure 6. Schematic diagram of TZG impairing NETs release through inhibiting PI3K-RAC2 signaling-mediated NADPH oxidase ROS production in MPS

study, our results indicated that the expression levels of inflammatory stimulators (IL-8, TNF-α) and biomarkers of NETs formation (dsDNA, MPO, CitH3, PAD4) were all significantly up-regulated in vastus medialis muscle around marked taut band or MTrPs of rats in the MPS model group, suggesting the successful establishment of MPS model, which were notably reversed by the treatment of TZG. Mechanically, our enriched PI3K-RAC2 signaling was closely related with NETs formation. NETs release has been indicated to require the involvement of proto-oncogenic serine/threonine kinase (Raf)/mitogen-activated protein kinase (MEK)/extracellular signal-regulated kinase (ERK) intracellular signaling. PI3K inhibition may subsequently suppress Raf-MEK-ERK signaling, thus blocking NETosis, while the activation of PI3K and its downstream ERK may play a vital role in triggering ROS-dependent NETs release at the condition of stimuli through promoting the binding of RAC2 and gp91 leading to P47 phosphorylation.[30] Moreover, RAC small GTPases are key regulators of ROS generation by activating NADPH oxidase in neutrophils, and RAC2 acts as an essential regulator of NETs formation in an isoform-specific manner.[15] Accordingly, both our transcriptomic data and experimental validations revealed that the p-PI3K/PI3K and p-P47/P47 ratios, and RAC2 protein expression were markedly increased in the MPS model group, but were efficiently reduced by TZG treatment.

In conclusion, our findings showed TZG may be a promising candidate drug for ameliorating the progression of MPS. We also provided an integrated network-based strategy for unveiling that TZG may impair NETs release through inhibiting PI3K-RAC2 signaling to reduce NADPH oxidase-originated ROS (Figure 6), which not only shed light into broadening the clinical indications of TZG, but benefit MPS therapy.

Limitations of the study

Firstly, we herein carried out the transcriptomic sequencing using the active MTrPs samples, which were collected from MPS rat model, but not from MPS patients because TZG has not been used for the treatment of MPS in clinics. Notably, our findings indicated that TZG may have a potential to alleviate the main symptoms and pathological changes of MPS, providing the experimental evidence for expanding the novel indications of this prescription.

Secondly, our established MPS animal model in the current study maximumly imitated clinical symptoms and etiology of MPS by combining continuous bluntly striking and eccentric-based exercises, however, some other triggers regarding neurotransmitter deregulation were missing. Therefore, this model may not be exactly equivalent to the clinical characteristics of MPS patients.

Thirdly, the chemical components contained in TZG haven't been clarified since TZG contains some animal drugs, such as *Scolopendridae* and *Elphe taeniura Cope*, the methodology for chemical identification of which still needs to be established.

We are looking for ways to overcome the previous limitations in our further study.

STAR★METHODS

Detailed methods are provided in the online version of this paper and include the following:

- KEY RESOURCES TABLE
- RESOURCE AVAILABILITY
  - Lead contact
  - Materials availability
  - Data and code availability
- EXPERIMENTAL MODEL AND STUDY PARTICIPANT DETAILS
  - Experimental animals

SUPPLEMENTAL INFORMATION

Supplemental information can be found online at https://doi.org/10.1016/j.isci.2023.108074.

ACKNOWLEDGMENTS

Scientific and technological innovation project of China Academy of Chinese Medical Sciences (No.CI2021A03808 & CI2023E001TS02); Technical Research and Development Project of Institute of Chinese Materia Medica (No.20211008); Fundamental Research Funds for the Central Public Welfare Research Institutes (No.ZZ15-YQ-029).

AUTHOR CONTRIBUTIONS

Conceptualization, Y.Zhang. and N.L.; Methodology, X.Liu., X.Mao., and Y. Liu.; Investigation, X.Liu., X.Mao., Y.Liu., W.Chen., and W.Li.; Writing-Original Draft, X.Liu., X.Mao., and Y.Liu.; Writing-Review and Editing, all authors; Funding Acquisition, Y.Zhang. and N.L.; Resources, Y.Zhang. and N.L.; Supervision, Y.Zhang. and N.L.

DECLARATION OF INTERESTS

The authors declare no competing interests.

INCLUSION AND DIVERSITY

We support inclusive, diverse, and equitable conduct of research.

Received: November 14, 2022
Revised: May 13, 2023
Accepted: September 25, 2023
Published: September 27, 2023

REFERENCES

1. Borg-Stein, J., and Iaccarino, M.A. (2014). Myofascial pain syndrome treatments. Phys. Med. Rehabil. Clin *2*, 357–374. https://doi.org/10.1016/j.pmr.2014.01.012.
2. Fleckenstein, J., Zaps, D., Rüger, L.J., Lehmeyer, L., Freiberg, F., Lang, P.M., and Irnich, D. (2010). Discrepancy between prevalence and perceived effectiveness of treatment methods in myofascial pain syndrome: results of a cross-sectional, nationwide survey. BMC Muscoskel. Disord. *11*, 32. https://doi.org/10.1186/1471-2474-11-32.
3. Simons, D.G. (2004). Review of enigmatic MTrPs as a common cause of enigmatic musculoskeletal pain and dysfunction. J. Electromyogr. Kinesiol. *14*, 95–107. https://doi.org/10.1016/j.jelekin.2003.09.018.
4. Li, X., Wang, R., Xing, X., Shi, X., Tian, J., Zhang, J., Ge, L., Zhang, J., Li, L., and Yang, K. (2017). Acupuncture for Myofascial Pain Syndrome: A Network Meta-Analysis of 33 Randomized Controlled Trials. Pain Physician *20*, E883–E902.
5. Simons, D.G., Hong, C.Z., and Simons, L.S. (2002). Endplate potentials are common to midfiber myofacial trigger points. Am. J. Phys. Med. Rehabil. *81*, 212–222. https://doi.org/10.1097/00002060-200203000-00010.
6. Hayashi, K., Ozaki, N., Kawakita, K., Itoh, K., Mizumura, K., Furukawa, K., Yasui, M., Hori, K., Yi, S.Q., Yamaguchi, t., and Sugiura, Y. (2011). Involvement of NGF in the rat model of persistent muscle pain associated with taut band. J. Pain *12*, 1059–1068. https://doi.org/10.1016/j.jpain.2011.04.010.
7. Galasso, A., Urits, I., An, D., Nguyen, D., Borchart, M., Yazdi, C., Manchikanti, L., Kaye, R.J., Kaye, A.D., Mancuso, K.F., and Viswanath, O. (2020). A Comprehensive Review of the Treatment and Management of Myofascial Pain Syndrome. Curr. Pain Headache Rep. *24*, 43. https://doi.org/10.1007/s11916-020-00877-5.
8. Criscuolo, C.M. (2001). Interventional approaches to the management of myofascial pain syndrome. Curr. Pain Headache Rep. *5*, 407–411. https://doi.org/10.1007/s11916-001-0051-9.
9. Liu, X.T., Chen, W.J., Liu, W., Li, P.H., Hu, Y.H., Lin, N., and Zhang, Y.Q. (2022). Mechanism of Tianhe Zhuifeng Ointment in treating rheumatoid arthritis with syndrome of internal obstruction and cold-dampness and compatibility principles based on "disease-syndrome-formula" association network. China J. Chin. Mater. Med. *47*, 4978–4986. (In Chinese). https://doi.org/10.19540/j.cnki.cjcmm.20220421.402.
10. LeBlanc, K.E., and LeBlanc, L.L. (2010). Musculoskeletal disorders. Prim. Care *37*, 389–406. https://doi.org/10.1016/j.pop.2010.02.006.

11. Shah, J.P., Thaker, N., Heimur, J., Aredo, J.V., Sikdar, S., and Gerber, L. (2015). Myofascial Trigger Points Then and Now: A Historical and Scientific Perspective. Pharm. Manag. *7*, 746–761. https://doi.org/10.1016/j.pmrj.2015.01.024.
12. Srbely, J.Z. (2010). New trends in the treatment and management of myofascial pain syndrome. Curr. Pain Headache Rep. *14*, 346–352. https://doi.org/10.1007/s11916-010-0128-4.
13. Akgul, O., Di Cesare Mannelli, L., Vullo, D., Angeli, A., Ghelardini, C., Bartolucci, G., Alfawaz Altamimi, A.S., Scozzafava, A., Supuran, C.T., and Carta, F. (2018). Discovery of Novel Nonsteroidal Anti-Inflammatory Drugs and Carbonic Anhydrase Inhibitors Hybrids (NSAIDs-CAIs) for the Management of Rheumatoid Arthritis. J. Med. Chem. *61*, 4961–4977. https://doi.org/10.1021/acs.jmedchem.8b00420.
14. Khan, N., and Smith, M.T. (2015). Neurotrophins and Neuropathic Pain: Role in Pathobiology. Molecules *20*, 10657–10688. https://doi.org/10.3390/molecules200610657.
15. Lim, M.B.H., Kuiper, J.W.P., Katchky, A., Goldberg, H., and Glogauer, M. (2011). Rac2 is required for the formation of neutrophil extracellular traps. J. Leukoc. Biol. *90*, 771–776. https://doi.org/10.1189/jlb.1010549.
16. Gavillet, M., Martinod, K., Renella, R., Wagner, D.D., and Williams, D.A. (2018). A key role for Rac and Pak signaling in neutrophil extracellular traps (NETs) formation defines a new potential therapeutic target. Am. J. Hematol. *93*, 269–276. https://doi.org/10.1002/ajh.24970.
17. Liu, S., Li, X., Zhou, X., Loor, J.J., Jiang, Q., Feng, X., Yang, Y., Lei, L., Du, X., Li, X., et al. (2022). β-Hydroxybutyrate impairs the release of bovine neutrophil extracellular traps through inhibiting phosphoinositide 3-kinase-mediated nicotinamide adenine dinucleotide phosphate oxidase reactive oxygen species production. J. Dairy Sci. *105*, 3405–3415. https://doi.org/10.3168/jds.2021-21174.
18. Zhang, M., Jin, F., Zhu, Y., and Qi, F. (2020). Peripheral FGFR1 Regulates Myofascial Pain in Rats via the PI3K/AKT Pathway. Neuroscience *436*, 1–10. https://doi.org/10.1016/j.neuroscience.2020.04.002.
19. Hiroki, C.H., Toller-Kawahisa, J.E., Fumagalli, M.J., Colon, D.F., Figueiredo, L.T.M., Fonseca, B.A.L.D., Franca, R.F.O., and Cunha, F.Q. (2019). Neutrophil Extracellular Traps Effectively Control Acute Chikungunya Virus Infection. Front. Immunol. *10*, 3108. https://doi.org/10.3389/fimmu.2019.03108.
20. Siegfried, M. (2020). How do muscle lesions such as latent and active trigger points influence central nociceptive neurons? J. Muscoskel. Pain *18*, 348–353. https://doi.org/10.3109/10582452.2010.502621.
21. Fleckenstein, J., Zaps, D., Rüger, L.J., Lehmeyer, L., Freiberg, F., Lang, P.M., and Irnich, D. (2010). Discrepancy between prevalence and perceived effectiveness of treatment methods in myofascial pain syndrome: results of a cross-sectional, nationwide survey. BMC Muscoskel. Disord. *11*, 32. https://doi.org/10.1186/1471-2474-11-32.
22. Duarte, F.C.K., West, D.W.D., Linde, L.D., Hassan, S., and Kumbhare, D.A. (2021). Re-Examining Myofascial Pain Syndrome: Toward Biomarker Development and Mechanism-Based Diagnostic Criteria. Curr. Rheumatol. Rep. *23*, 69. https://doi.org/10.1007/s11926-021-01024-8.
23. Ramon, S., Gleitz, M., Hernandez, L., and Romero, L.D. (2015). Update on the efficacy of extracorporeal shockwave treatment for myofascial pain syndrome and fibromyalgia. Int. J. Surg. *24*, 201–206. https://doi.org/10.1016/j.ijsu.2015.08.083.
24. Romero-Morales, C., Bravo-Aguilar, M., Abuín-Porras, V., Almazán-Polo, J., Calvo-Lobo, C., Martínez-Jiménez, E.M., López-López, D., and Navarro-Flores, E. (2021). Current advances and novel research on minimal invasive techniques for musculoskeletal disorders. Dis. Mon. *67*, 101210. https://doi.org/10.1016/j.disamonth.2021.101210.
25. Huang, Q.M., Ye, G., Zhao, Z.Y., Lv, J.J., and Tang, L. (2013). Myoelectrical activity and muscle morphology in a rat model of myofascial trigger points induced by blunt trauma to the vastus medialis. Acupunct. Med. *31*, 65–73. https://doi.org/10.1136/acupmed-2012-010129.
26. Alvarez, D.J., and Rockwell, P.G. (2002). Trigger points: diagnosis and management. Am. Fam. Physician *65*, 653–660.
27. Munrós, J., Tàssies, D., Reverter, J.C., Martin, L., Pérez, A., Carmona, F., and Martínez-Zamora, M.Á. (2019). Circulating Neutrophil Extracellular Traps Are Elevated in Patients With Deep Infiltrating Endometriosis. Reprod. Sci. *26*, 70–76. https://doi.org/10.1177/1933719118757682.
28. Castanheira, F.V.S., and Kubes, P. (2019). Neutrophils and NETs in modulating acute and chronic inflammation. Blood *133*, 2178–2185. https://doi.org/10.1182/blood-2018-11-844530.
29. Podolska, M.J., Mahajan, A., Knopf, J., Hahn, J., Boeltz, S., Munoz, L., Bilyy, R., and Herrmann, M. (2018). Autoimmune, rheumatic, chronic inflammatory diseases: Neutrophil extracellular traps on parade. Autoimmunity *51*, 281–287. https://doi.org/10.1080/08916934.2018.1519804.
30. Zheng, S., Wang, S., Zhang, Q., Zhang, Z., and Xu, S. (2020). Avermectin inhibits neutrophil extracellular traps release by activating PTEN demethylation to negatively regulate the PI3K-ERK pathway and reducing respiratory burst in carp. J. Hazard Mater. *389*, 121885. https://doi.org/10.1016/j.jhazmat.2019.121885.
31. Li, L.H., Huang, Q.M., Barbero, M., Liu, L., Nguyen, T.T., Beretta-Piccoli, M., Xu, A.L., and Ji, L.J. (2019). Quantitative proteomics analysis to identify biomarkers of chronic myofascial pain and therapeutic targets of dry needling in a rat model of myofascial trigger points. J. Pain Res. *12*, 283–298. https://doi.org/10.2147/JPR.S185916.
32. Simons, D.G., Travell, T.G., and Simons, L.S. (1999). Myofascial Pain and Dysfunction: The Trigger Point Manual, *Vol. 1*, 2nd ed. (Lippincott, Williams & Wilkins).
33. Jin, F., Zhao, L., Hu, Q., and Qi, F. (2020). Peripheral EphrinB1/EphB1 signalling attenuates muscle hyperalgesia in MPS patients and a rat model of taut band-associated persistent muscle pain. Mol. Pain *16*, 1744806920984079. https://doi.org/10.1177/1744806920984079.
34. Li, W., Wang, K., Liu, Y., Wu, H., He, Y., Li, C., Wang, Q., Su, X., Yan, S., Su, W., et al. (2022). A Novel Drug Combination of Mangiferin and Cinnamic Acid Alleviates Rheumatoid Arthritis by Inhibiting TLR4/NFκB/NLRP3 Activation-Induced Pyroptosis. Front. Immunol. *13*, 912933. https://doi.org/10.3389/fimmu.2022.912933.
35. Mao, X., Li, W., Chen, W., Li, Y., Wang, Q., Wang, X., Pi, Z., Wang, D., Xu, H., Guo, Q., et al. (2020). Exploring and characterizing a novel combination of paeoniflorin and talatizidine for the treatment of rheumatoid arthritis. Pharmacol. Res. *153*, 104658. https://doi.org/10.1016/j.phrs.2020.104658.
36. Shinoda, K., Hruby, V.J., and Porreca, F. (2007). Antihyperalgesic effects of loperamide in a model of rat neuropathic pain are mediated by peripheral delta-opioid receptors. Neurosci. Lett. *411*, 143–146. https://doi.org/10.1016/j.neulet.2006.10.027.
37. Bardin, L., Malfetes, N., Newman-Tancredi, A., and Depoortère, R. (2009). Chronic restraint stress induces mechanical and cold allodynia., and enhances inflammatory pain in rat: Relevance to human stress-associated painful pathologies. Behav. Brain Res. *205*, 360–366. https://doi.org/10.1016/j.bbr.2009.07.005.
38. Huang, Q.M., Lv, J.J., Ruanshi, Q.M., and Liu, L. (2015). Spontaneous electrical activities at myofascial trigger points at different stages of recovery from injury in a rat model. Acupunct. Med. *33*, 319–324. https://doi.org/10.1136/acupmed-2014-010666.
39. Zhang, Y., Li, X., Shi, Y., Chen, T., Xu, Z., Wang, P., Yu, M., Chen, W., Li, B., Jing, Z., et al. (2023). ETCM v2.0: An update with comprehensive resource and rich annotations for traditional Chinese medicine. Acta Pharm Sin B *13*, 2559–2571.
40. Szklarczyk, D., Franceschini, A., Wyder, S., Forslund, K., Heller, D., Huerta-Cepas, J., Simonovic, M., Roth, A., Santos, A., Tsafou, K.P., et al. (2015). STRING v10: protein-protein interaction networks, integrated over the tree of life. Nucleic Acids Res. *43*, D447–D452. https://doi.org/10.1093/nar/gku1003.
41. Wixon, J., and Kell, D. (2000). The Kyoto encyclopedia of genes and genomes—KEGG. Yeast *17*, 48–55. https://doi.org/10.1002/(SICI)1097-0061(200004)17:1<48::AID-YEA2>3.0.CO;2-H.
42. Gillespie, M., Jassal, B., Stephan, R., Milacic, M., Rothfels, K., Senff-Ribeiro, A., Griss, J., Sevilla, C., Matthews, L., Gong, C., et al. (2022). The reactome pathway knowledgebase 2022. Nucleic Acids Res. *50*, D687–D692. https://doi.org/10.1093/nar/gkab1028.

STAR★METHODS

KEY RESOURCES TABLE

REAGENT or RESOURCE	SOURCE	IDENTIFIER
Antibodies		
Rabbit anti-NGF (dilution 1:1000, monoclonal)	Hangzhou HUABIO Biotechnology Co. LTD. Hangzhou, China	ET1606-29
Rabbit anti-BDNF (dilution 1:1000, monoclonal)	Hangzhou HUABIO Biotechnology Co. LTD. Hangzhou, China	ET1606-42
Rabbit anti-NE (dilution 1:1000, monoclonal)	Wuhan ABclonal Technology Co. LTD. Antibody	A13015 RRID: AB_2759862
Rabbit anti-PAD4 (dilution 1:500, monoclonal)	Abcam, Co. LTD. Cambridge, UK	ab214810
Rabbit anti-P47 (dilution 1:1000, polyclonal)	Hangzhou HUABIO Biotechnology Co. LTD. Hangzhou, China	ER64501
Rabbit anti-p-P47 (dilution 1:1000, polyclonal)	Affinity Biosciences LTD. Melbourne, Australia	AF3167 RRID: AB_2834599
Rabbit anti-PI3K (dilution 1:500, monoclonal)	Cell signaling technology LTD. Boston, USA	4249s
Rabbit anti-p-PI3K (dilution 1:1000, polyclonal)	Affinity Biosciences LTD. Melbourne, Australia	AF7421 RRID: AB_2843861
Rabbit anti-RAC2 (dilution 1:1000, polyclonal)	Affinity Biosciences LTD. Melbourne, Australia	DF6273 RRID: AB_2838239
Mouse anti-β-actin (dilution 1:1000, monoclonal)	Wuhan Boster Biological Technology Co. LTD. Antibody	BM0627 RRID: AB_2814866
Horseradish peroxidase-conjugated anti-rabbit IgG	Wuhan Boster Biological Technology Co. LTD. Antibody	BA1054 RRID: AB_2734136
Horseradish peroxidase-conjugated anti-mouse IgG	Wuhan Boster Biological Technology Co. LTD. Antibody	BA1050 RRID: AB_2904507
CitH3 (dilution 1:1000)	Abcam, Cambridge	Ab176842 RRID: AB_2493104
Fluorescein isothiocyanate conjugated donkey anti-rabbit IgG (dilution 1:200)	Servicebio, Wuhan, China	GB22403 RRID: AB_2868508
Chemicals, peptides, and recombinant proteins		
PI	Beyotime, Shanghai, China	ST511
CD31	Abcam, Cambridge, UK	Ab182981 RRID: AB_2920881
Tianhe Zhuifeng Gao	Tianhe, Guilin, China	20210806
Shexiang Zhuanggu Gao	Tianhe, Guilin, China	20210709
Critical commercial assays		
RNeasy Mini Kit (250)	Qiagen, Dusseldorf, Germany	#74106
DAB color development kit	Servicebio, Wuhan, China	G1212-200
AB-PAS dying reagent kit	Solarbio, Beijing, China	G1285
CitH3 elisa kit	Meimian, Wuhan China	MM-0741R2
TNF-α elisa kit	Meimian, Wuhan China	MM-0180R2
IL-8 elisa kit	Meimian, Wuhan China	MM-0175R2
MPO elisa kit	Meimian, Wuhan China	MM-0337R2
dsDNA elisa kit	Maokang, Shanghai, China	MF0781
Ready-to-use UltraSensitive s-p hypersensitivity kit	Maixin, Fuzhou, China	KIT-9706
Deposited data		
Raw data of gene expression microarray	This paper	GEO: GSE217118
Experimental models: Organisms/strains		
Sprague-Dawley rats	Guangdong Medical Laboratory Animal Center	SCXK2018-0002

(*Continued on next page*)

Continued

REAGENT or RESOURCE	SOURCE	IDENTIFIER
Software and algorithms		
ImageJ software	National Institutes of Health	Version 7.0
Graphprism	GraphPad, California, USA	Version 6.0
Other		
Treadmill	TOMOS, New Jersey, USA	YS-100
Von Frey filaments	Stoelting, Wood Dale, IL	NC12775
EMG detector instrument	TECHMAN, Sichuan, China	BL-420S
Optical microscope with a digital camera	MSHOT, Guangzhou, China	ML31
Agilent Bioanalyzer 5400	Agilent technologies, Santa Clara, CA, US	5400
NanoDrop One spectrophotometer	Thermo Fisher Scientific, Massachusetts, US	NanoDrop One
Agilent Technologies 2100 Bioanalyzer	Agilent technologies, Santa Clara, CA, US	2100
Illumina NovaSeq 6000 sequence platform	Illumina, California, US	Illumina NovaSeq 6000
Fluorescence microscope	MSHOT, Guangzhou, China	MF53
Multiskoun GO enzyme-labeled instrument	Thermo Fisher Scientific, Waltham, MA USA	Multiskoun GO

RESOURCE AVAILABILITY

Lead contact

Further information and requests for resources and reagents should be directed to and will be fulfilled by the lead contact, Yanqiong Zhang (yqzhang@icmm.ac.cn).

Materials availability

This study did not generate new unique reagents.

Data and code availability

- Raw data of gene expression microarray have been deposited at NCBI Gene Expression Omnibus and publicly available as of the date of publication. Accession numbers are listed in the key resources table. All the data reported in this paper will be shared by the lead contact upon request.
- This paper does not report original code.
- Any additional information required to reanalyze the data reported in this paper is available from the lead contact upon request.

EXPERIMENTAL MODEL AND STUDY PARTICIPANT DETAILS

Experimental animals

Forty-eight male SD rats of 6∼8 weeks old, weighting 180∼200g, were purchased from Guangdong Medical Laboratory Animal Center (Production license no.: SCXK2018-0002) and used in this study. All rats were housed conventionally in a specific pathogen-free animal facility under a 12 h light-dark cycle, with a controlled temperature of 22∼24°C and 20–30% humidity, and provided with food and water *ad libitum*. All efforts were made to minimize sacrificed animal numbers based on common sense for deciding a suitable sample size, and procedures throughout experiments were carried out in compliance with the ethical standards of the Center for Laboratory Animal Care, China Academy of Chinese Medical Sciences, and Institutional Animal Care and Use Committee of Guangzhou Medical University with the ethical proof No. 2017-198.

Animal models of MTrPs and treatment

All enrolled rats were divided randomly and evenly into six groups (n = 8 per group), including normal control group, model group, TZG-L treatment group (Lot No. 20210806, Tianhe, Guilin, China), TZG-M treatment group, TZG-H treatment group, and positive medicine named SXZG treatment group (Lot No. 20210709, Tianhe, Guilin, China). Rats in the normal control group were fed conventionally without any intervention, and rat models of MTrPs were established by blunt striking injury to the left vastus medialis in combined with eccentric exercise for 8 weeks, along with 2 weeks of recovery, according to the previous studies.[25,31] In details, rats were anesthetized by abdominal aortic method using 2% pentobarbital sodium after weighing, then fixed at the bottom of the percussion apparatus, followed by hitting with a stick of 2.352 J kinetic energy, which was achieved through a 1200 g stick dropping freely from a height of 21cm on the site of left vastus medialis marked on the skin. Then, rats were anesthetized once again to avoid ankylenteron. The next day, rats ran on a treadmill (Lot No. YS-100,

TOMOS, New Jersey, USA) with a downward angle of −16°, and the speed was gradually increased to 16 m/min over 1.5 h. General health conditions of rats during the procedures, such as weight, limb movement and taut band changes, were monitored weekly. Subsequently, rats were arranged to rest for the remaining 5 days a week without any intervention (Figure 1A). The presence or absence of taut band was assessed on the affected hindlimb in each animal using the flat palpation method described by Travell et al. after complete dissection of the skin and underlying fascia.[32] Active MTrPs were identified by referring to the 2017 International Consensus on Diagnostic Standards for Trigger Points of MPS: 1) Rapid decrease of mechanical sensitivity on taut bands; 2) Ability to elicit LTRs after acupuncture needle insertion into the tender spot; 3) Appearance of tender spots or contracture modules in a palpable tant bands.[33]

For drug delivery, low-, middle-, high doses of TZG extractum and positive drug SXZG extractum were externally applied to the MTrPs from the third day till the seventh day during each experimental cycle since the first week of MTrPs modeling till the end, complemented with another 2 weeks pure treatment to form a total of 10 weeks treatment. Concretely, TZG or SXZG were evenly smeared to the skin regions around 6 × 7 cm of MTrPs after hair removing and cleaning. Then, massaging treatment areas for 5 min to promote medication absorption, and fixed with gauze. Dosage selections for low-, middle-, high doses of TZG extractum were 299.52 mg/kg, 599.04 mg/kg and 1198.08 mg/kg, respectively, which were equivalent to 1, 2 and 4 times of clinical treatment doses, and that of SXZG extractum was 1 time of clinical usage at the dosage of 299.52 mg/kg. Rats in the normal control group and model group were applied with the same volume of saline.

METHOD DETAILS

Assessment of pain sensitivity

Pain thresholds that include mechanical hyperalgesia and acetone-induced cold allodynia were examined according to our previous studies.[34,35] In details, the mechanical sensitivity of the plantar surface of the hind paw was evaluated by applying von Frey filaments (Lot No. NC12775, Stoelting, Wood Dale, IL). The von Frey hairs were pressed against the plantar surface of the hind paw and withdrawal response frequency was measured using an up-down method.[36] Acetone-induced cold allodynia was measured by dropping 50 μL of acetone with an injector with a blunted needle into the middle of the plantar face of a hind paw. Acetone was applied three times to each rat with a 5-minite interval. Responses were monitored and scored during 1 min after acetone application and were graded according to a 3-point scale, as presented by Flatters and Bennett: 0 (no response); 1 (quick withdrawal); 2 (prolonged withdrawal, flicking or stamping of the paw); 3 (prolonged withdrawal, repeated flicking or stamping of the paw). The final score of each rat were calculated by averaging the sum of three times of scores.[37]

Electromyography analysis

The location of MTrPs was determined by referring to the method previously described by Huang et al.[38] Briefly, the left vastus medialis with blunt trauma in each rat was completely exposed after anesthesia with an intraperitoneal injection of 2% pentobarbital sodium, and the taut band was palpated and marked on the skin. A possible MTrP can be identified if LTR appeared immediately after the first needle inserting into the tail of the rats as a reference electrode, and the second needle into the marked taut band. Then, a third electrode was inserted longitudinally into the possible MTrP, 3 to 5 mm distant form the other electrode. Three needles were all connected to the EMG detector instrument (Lot No. BL-420S, TECHMAN, Sichuan, China) for detecting SEA, which suggested the possible MTrP to be an active MTrP after SEA observed.

Histological analysis and observation

Before being sacrificed, vastus medialis muscle around marked taut band of rats were acquired after anesthetized with an intraperitoneal injection of 2% pentobarbital sodium. Obtained tissues were equally divided into two parts, one which was immediately frozen in liquid nitrogen and stored at −80°C for further western blot analysis, immunohistochemical analysis and immunofluorescence, the other fixed in 4% paraformaldehyde at 4°C for 24 h for staining. Subsequently, specimens fixed were processed according to routine procedures, including dehydration, paraffin embedding, and sectioning. Sections at a thickness of 4 mm were placed on the slide, and stained with H&E after being dewaxed. Then, slices were dehydrated in gradient concentration of ethanol (70–100%) and xylene, and covered with cover slips. Histological images of slices were captured using an optical microscope with a digital camera (Lot No. ML31, MSHOT, Guangzhou, China).

Alcian PAS staining

Following the routine procedures of paraffin being dewaxed, slices were dehydrated in gradient concentration of ethanol (75–100%), and then examined using AB-PAS dying reagent kit (Lot No. G1285, Solarbio, Beijing, China) according to its protocols. Images of slices were captured using an optical microscope with a digital camera (Lot No. ML31, MSHOT, Guangzhou, China).

Microarray and differential data analysis

Microarray analysis was carried out to obtain DEGs by comparing gene expression profilings among different groups. The active MTrPs samples were collected from rats of each group and then transferred immediately into liquid nitrogen after anesthesia for further analysis. Total RNA samples were extracted from tissues using RNeasy Mini Kit (250) (Lot No. #74106, Qiagen, Dusseldorf, Germany), inspected of quality by Agilent Bioanalyzer 5400 (Agilent technologies, Santa Clara, CA, US), and quantified using NanoDrop One spectrophotometer (Thermo Fisher Scientific, Massachusetts, US). After proceeding using an Agilent Technogies 2100 Bioanalyzer (Agilent technologies, Santa Clara,

CA, US), microarray analysis of full transcriptome was conducted using Illumina NovaSeq 6000 sequence platform (Illumina, California, US) according to the manufacturer's instructions. Genes with log2 ratio ≥ 1 or log2 ratio ≤ -1 and P-value <0.05 were selected for data analysis. Hierarchical clustering was performed using Agilent GeneSpring GX software to identify DEGs according to the heatmap package in R (version 1.0.2, R Core Team, Vienna, Austria), then followed by the Cluster analysis (Cluster 3.0) on the basis of Euclidean distance. MPS-related genes (DEGs of MPS model group vs. control group) and TZG effective genes (DEGs of TZG treatment group vs. MPS model group) were identified. Raw data of gene expression microarray was uploaded in the National Center of Biotechnology Information (NCBI) Gene Expression Omnibus (GEO: GSE217118).

Network construction and analysis

"MPS-related gene–TZG-effective gene" interaction network was constructed using links between MPS-related genes and TZG effective genes, which were obtained through the public databases ETCM v2.0 (Encyclopedia of Traditional Chinese Medicine, version 2.0, http://www.tcmip.cn/ETCM2/front/#/)[39] and STRING (Search Tool for Known and Predicted Protein-Protein Interactions, version 10.0, http://string-db.org/),[40] and visualized by Navigator software (Version 2.2.1). Hub genes were screened by calculating their topological feature of degree, the value of which were higher than twice the median. Using the direct interaction information of those hub genes, the shortest path value from each TZG-effective gene to MPS-related gene was calculated and sorted to evaluate the strength of the association between TZG-effective genes and MPS-related genes. Then, functional enrichment analysis was performed based on Kyoto Encyclopedia of Genes and Genomes (KEGG, http://www.genome.jp/kegg/) database,[41] and Reactome Pathway Database (https://reactome.org/) database.[42] The pathways enriched by the major TZG-effective genes, the shortest path values to MPS-related genes of which were lower than the corresponding median value were selected for further investigation.

Western blot analysis

To investigate the regulatory effects of TZG on expression levels of MPS-related genes, and candidate therapeutics targets in MTrPs samples, vastus medialis muscle around MTrPs and spinal dorsal horn, Western blot analysis was performed as described previously.[34,35] The following primary antibodies were applied: anti-NGF, anti-BDNF, anti-NE, anti-PAD4, anti-P47, anti-p-P47, anti- PI3K, anti-p-PI3K, anti-RAC2 and anti-β-actin. After incubated at 4°C overnight, the blocked membranes were reacted with the corresponding second-antibodies, including horseradish peroxidase-conjugated anti-rabbit IgG (Lot No. BA1054, Boster, Wuhan, China) and horseradish peroxidase-conjugated anti-mouse IgG (Lot No. BA1050, Boster, Wuhan, China). The western blot signals were visualized by an enhanced chemiluminescence method, and quantified using Image J software (Version 7.0).

Immunofluorescence

After dewaxing and rehydrating, paraffin sections of vastus medialis muscle around MTrPs were subjected to immunofluorescence staining with the primary antibody against CitH3 (Lot No. Ab176842, Abcam, Cambridge, UK. 1:1000) at 4°C overnight, then with fluorescein isothiocyanate conjugated donkey anti-rabbit IgG (H&L) (Lot No. GB22403, Servicebio, Wuhan, China. 1:200) for 1 h at room temperature on the next day. PI (Lot No. ST511, Beyotime, Shanghai, China) was used to display the nucleus. The slides were observed under a fluorescence microscope (Lot No. MF53, MSHOT, Guangzhou, China), and the fluorescence intensity was quantified using Image J software (Version 7.0).

Immunohistochemistry

The immunohistochemistry analysis of tissues was performed using Ready-to-use UltraSensitive s-p hypersensitivity kit (Rabbit) (Lot No. KIT-9706, Maixin, Fuzhou, China) according to manufactures' instructions. The primary antibody against CD31 (Lot No. Ab182981, Abcam, Cambridge, UK. 1:100) and NE were applied, followed by tissues incubated with DAB color development kit (Lot No. G1212-200, Servicebio, Wuhan, China) for 5 min, and stained with hematoxylin for 1 min. After dehydration and clearing, the sealed slides were observed under an optical microscope. Immunostained areas were quantified using Image J software (Version 7.0).

ELISA

Before sacrifice, the blood serum of rats was collected by abdominal aortic method after being anesthesia, and centrifuged at 3000 rpm for 15 min to obtain supernatant for detecting expression levels of CitH3 (Lot No. MM-0741R2, Meimian, Wuhan China), TNF-α (Lot No. MM-0180R2, Meimian, Wuhan China), IL-8 (Lot No. MM-0175R2, Meimian, Wuhan China), MPO (Lot No. MM-0337R2, Meimian, Wuhan China) and dsDNA (Lot No. MF0781. Maokang, Shanghai, China). In addition, homogenates of MTrPs were centrifuges for 20 min at 10000 rpm, and then the supernatants were recentrifuged for 30 min at 15000 rpm at 4°C, the resulting supernatants were used for samples of ELISA to detect TNF-α, IL-8 and MPO. All procedures were performed in accordance with the manufacturer's instructions using Multiskoun GO enzyme-labeled instrument (Thermo Fisher Scientific, Waltham, MA USA).

QUANTIFICATION AND STATISTICAL ANALYSIS

All statistical analyses were calculated using Graphprism version 6.0 (GraphPad, California, USA) by one-way analysis of variance, followed by a Lest Significant Difference (LSD) test. The continuous data were shown with mean ± standard deviation. All experiments were performed in triplicate. Differences were considered statistically significant when the value of P was less than 0.05.